

atoms. These results suggest that it should be possible to prepare new materials with different structures from mixed phosphate-phosphinate or phosphite systems. This work is in progress.

Acknowledgment. We gratefully acknowledge support for this work by the Robert A. Welch Foundation under Grant No. A673.

The single-crystal diffractometer was purchased under DOD Grant No. N-00014-86-G-0194.

Supplementary Material Available: Table SI, giving experimental crystallographic details and anisotropic thermal parameters (4 pages); Table SII, listing calculated and observed structure amplitudes (29 pages). Ordering information is given on any current masthead page.

Contribution from the Dipartimento di Chimica, Università di Firenze, Via Maragliano 75/77, 50144 Firenze, Italy, Laboratoire de Chimie des Métaux de Transition, Université Pierre et Marie Curie, 75230 Paris, France, and Departament de Química Inorgànica, Facultat de Química, Universitat de València, C/Dr. Moliner 50, Burjassot, 46100 València, Spain

Oxalato and Squarate Ligands in Nickel(II) Complexes of Tetraazacycloalkanes. Solution and Solid-State Studies. Crystal and Molecular Structures of (μ -Oxalato)bis[(1,7-dimethyl-1,4,7,10-tetraazacyclododecane)nickel(II)] Perchlorate Dihydrate and of Bis[diaquo(1,4,7,10-tetraazacyclododecane)nickel(II)] Squarate Diperchlorate

Andrea Bencini,^{1a} Antonio Bianchi,^{*1a} Enrique Garcia-España,^{*1b} Yves Jeannin,^{1c} Miguel Julve,^{*1b} Victor Marcelino,^{1b} and Michèle Philoche-Levisalles^{1c}

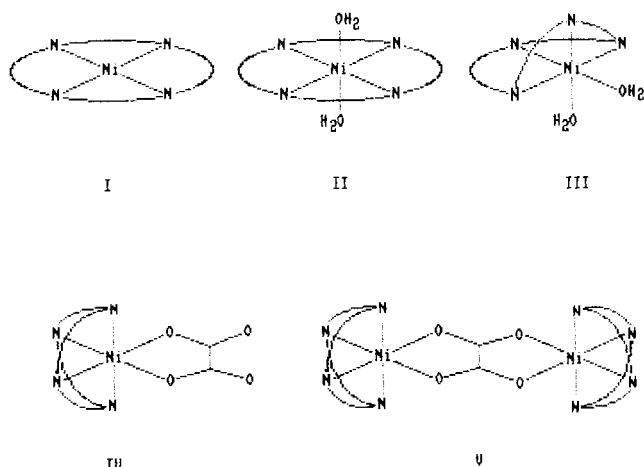
Received May 12, 1989

Three new nickel(II) complexes of formula $[\text{Ni}_2(\text{Me}_2\text{cyclen})_2\text{ox}](\text{ClO}_4)_2 \cdot 2\text{H}_2\text{O}$ (1), $[\text{Ni}_2(\text{cyclen})_2\text{ox}](\text{NO}_3)_2$ (2), and $[\text{Ni}(\text{cyclen})(\text{H}_2\text{O})_2](\text{C}_4\text{O}_4)(\text{ClO}_4)_2$ (3), where $\text{Me}_2\text{cyclen} = 1,7$ -dimethyl-1,4,7,10-tetraazacyclododecane, $\text{cyclen} = 1,4,7,10$ -tetraazacyclododecane, ox^{2-} = the oxalate anion, and $\text{C}_4\text{O}_4^{2-}$ = the dianion of 3,4-dihydroxy-3-cyclobutene-1,2-dione (squarate), have been synthesized. The crystal and molecular structures of 1 and 3 have been solved at 298 K by single-crystal X-ray analyses. 1 crystallizes in the monoclinic system, space group $P2_1/n$, with $a = 22.815$ (15) Å, $b = 10.713$ (1) Å, $c = 7.506$ (3) Å, $\beta = 97.85$ (3)°, $Z = 2$, and $R = 0.0415$. 3 crystallizes in the orthorhombic system, space group $P2_1cn$, with $a = 11.124$ (3) Å, $b = 11.461$ (3) Å, $c = 5.735$ (6) Å, $Z = 4$, and $R = 0.0345$. The structure of 1 consists of centrosymmetrical μ -oxalato-bridged nickel(II) binuclear units $[\text{Ni}_2(\text{Me}_2\text{cyclen})_2\text{ox}]^{2+}$ with noncoordinated perchlorate anions and water molecules. The tetraazamacrocycle adopts a folded conformation around the nickel atom, which is 6-coordinated in an octahedral distorted arrangement: the Ni-N distances are in the range 2.050 (2)–2.154 (3) Å, and the Ni-O(ox) distances are 2.095 (2) and 2.102 (2) Å. The oxalate ion acts as a bis-bidentate ligand between two nickel(II) ions. The structure of 3 is made up of $[\text{Ni}(\text{cyclen})(\text{H}_2\text{O})_2]^{2+}$ units and noncoordinated squarate and perchlorate anions. The tetraazamacrocycle adopts a folded conformation to produce a cis-pseudooctahedral geometry at each nickel atom. The configuration of the four nitrogen atoms is such that the hydrogen atoms attached to them are on the same side with respect to the idealized macrocyclic plane. Coordinated water molecules and squarate oxygen atoms are linked by hydrogen bonds. Intramolecular antiferromagnetic spin-exchange coupling between the two nickel(II) ions is observed for complexes 1 ($J = -34 \text{ cm}^{-1}$; $g = 2.30$) and 2 ($J = -35 \text{ cm}^{-1}$; $g = 2.15$) (J being the parameter of the exchange Hamiltonian $\hat{H} = -J\hat{S}_A\hat{S}_B$). The thermodynamic parameters of the equilibrium $[\text{Ni}(\text{L})]^{2+} + \text{ox}^{2-} = [\text{Ni}(\text{L})\text{ox}]$ where L = cyclam, cyclen, and Me_2cyclen have been determined by potentiometric and microcalorimetric measurements in aqueous solution at 25 °C in 0.1 mol dm^{-3} KNO_3 . The values of ΔG° found for the addition of the oxalate anion to $[\text{Ni}(\text{cyclen})]^{2+}$ and $[\text{Ni}(\text{Me}_2\text{cyclen})]^{2+}$ are equal within experimental error ($\Delta G^\circ = -5.6$ (1) and -5.7 (1) kcal mol^{-1} , respectively). A greater enthalpy of reaction has been found for $[\text{Ni}(\text{Me}_2\text{cyclen})]^{2+}$ ($\Delta H^\circ = -2.9$ (1) kcal mol^{-1}) than for $[\text{Ni}(\text{cyclen})]^{2+}$ ($\Delta H^\circ = -2.4$ (1) kcal mol^{-1}). The addition of oxalate to $[\text{Ni}(\text{cyclam})]^{2+}$ (69% square, 29% *trans*-diaquo, 2% *cis*-diaquo forms) is an enthalpy-driven reaction ($\Delta G^\circ = -3.8$ (1) kcal mol^{-1} and $\Delta H^\circ = -3.8$ (1) kcal mol^{-1}). From these values, the thermodynamic parameters for the reaction of oxalate with each one of the three forms have been calculated and discussed.

Introduction

In a recent paper,² we have reported the synthesis, crystal structure, and magnetic properties of the mixed-ligand complex $[\text{Ni}_2(\text{cyclam})_2\text{ox}](\text{NO}_3)_2$ (cyclam = 1,4,8,11-tetraazacyclotetradecane and ox^{2-} = oxalate anion). In this complex, oxalate acts as a bis-bidentate ligand bridging two $[\text{Ni}(\text{cyclam})]^{2+}$ units. In the same paper, we have also reported the equilibrium constants for the reactions $[\text{Ni}(\text{cyclam})]^{2+} + \text{ox}^{2-} = [\text{Ni}(\text{cyclam})\text{ox}]$ and $[\text{Ni}(\text{cyclam})\text{ox}] + [\text{Ni}(\text{cyclam})]^{2+} = [\text{Ni}_2(\text{cyclam})_2\text{ox}]^{2+}$. Aqueous solutions of $[\text{Ni}(\text{cyclam})]^{2+}$ are composed by an equilibrium mixture involving a square diamagnetic and two octahedral paramagnetic (both *cis*- and *trans*-diaquo) species (Chart I), the *cis*-diaquo complex being present in a very low percentage.³ The oxalate anion can coordinate to $[\text{Ni}(\text{cyclam})]^{2+}$ in a bidentate fashion when the tetraazamacrocyclic ligand is arranged in a folded conformation (Chart I, drawing IV), so that only the *cis*-diaquo

Chart I



form (Chart I, drawing III) exhibits the right conformation to allow such a coordination. The formation of the oxalato-bridged complex $[\text{Ni}_2(\text{cyclam})_2\text{ox}]^{2+}$ gives rise, owing to the particular

(1) (a) Università di Firenze. (b) Universitat de València. (c) Université Pierre et Marie Curie.
 (2) Battaglia, L. P.; Bianchi, A.; Bonamartini Corradi, A.; Garcia-España, E.; Julve, M.; Micheloni, M. *Inorg. Chem.* 1988, 27, 4174.
 (3) Billo, E. J. *Inorg. Chem.* 1984, 23, 2223.

ability of oxalate ligand to propagate electronic effects, to a relatively strong intramolecular antiferromagnetic interaction between the two single-ion triplet states.

It is well-known that variations in the structural features of the macrocyclic ligands induce important changes in the chemical properties of their metal complexes. For instance, in contrast with what has been observed for the 14-membered macrocyclic ligand cyclam,³⁻¹¹ the smaller 12-membered cyclen (1,4,7,10-tetraazacyclododecane) is almost unable to form, in aqueous solution, nickel(II) complexes with a planar arrangement of the macrocyclic ring¹²⁻¹⁴ (Chart I, drawings I and II), and except under particular conditions,¹³ it forms only the *cis*-diaquo complex (Chart I, drawing III). Thereby, [Ni(cyclen)]²⁺ is "well-disposed" to undergo coordination by bidentate ligands. The stability constant for [Ni(cyclen)(H₂O)₂]²⁺ is lower, by a factor of 10⁴, than that for *cis*-[Ni(cyclam)(H₂O)₂]²⁺.^{11,12} Similarly, a somewhat different chemical behavior in the coordination of bidentate ligands to [Ni(cyclen)]²⁺ and [Ni(cyclam)]²⁺ is to be expected.

In this paper, we present the results of a thermodynamic study, carried out by potentiometric and microcalorimetric techniques, on the interaction of oxalate and squarate anions with these complexes. The results herein reported for [Ni(cyclam)]²⁺ complete a previous study. Moreover, this investigation has been extended to [Ni(Me₂cyclen)]²⁺ (Me₂cyclen = 1,7-dimethyl-1,4,7,10-tetraazacyclododecane) in order to analyze the changes in chemical behavior brought about by the insertion of hindering groups on the donor atoms of the 12-membered macrocyclic ligand. The magnetic properties of the complexes [Ni₂(cyclen)₂ox](NO₃)₂ (2) and [Ni₂(Me₂cyclen)₂ox](ClO₄)₂·2H₂O (1) as well as the crystal and molecular structures of (1) and [Ni(cyclen)(H₂O)₂]₂(C₄O₄)(ClO₄)₂ (3) are also reported and discussed.

Experimental Section

Materials. Nickel(II) perchlorate hexahydrate, nickel(II) nitrate hexahydrate, oxalic acid dihydrate, sodium oxalate, potassium nitrate, squaric acid, lithium hydroxide monohydrate, 1,4,7,10-tetraazacyclododecane (cyclen), and 1,4,8,11-tetraazacyclotetradecane (cyclam) are available as commercial products and were used as received. 1,7-Dimethyl-1,4,7,10-tetraazacyclododecane (Me₂cyclen) was synthesized as reported in the literature.¹⁴

[Ni(Me₂cyclen)](NO₃)₂. A solution of Ni(NO₃)₂·6H₂O (1 mmol) in 5 cm³ of methanol was added to a hot solution (25 cm³) of Me₂cyclen (1 mmol) in butanol. The complex separated immediately as a mauve powder. The product was filtered, washed with ethanol and then with diethyl ether, and dried in vacuo. Anal. Calcd for C₁₀H₂₄N₆NiO₆: C, 31.36; H, 6.32; N, 21.94. Found: C, 31.6; H, 6.4; N, 22.0.

[Ni(Me₂cyclen)](ClO₄)₂. A boiling solution of Ni(ClO₄)₂ (1 mmol) in 5 cm³ of absolute ethanol was added to a boiling solution of Me₂cyclen (1 mmol) in 25 cm³ of absolute ethanol in a N₂ atmosphere. An orange microcrystalline powder immediately formed. The product was filtered, washed with absolute ethanol, and dried in vacuo at 50 °C. (*Caution!* Perchlorate salts of metal complexes can be explosive and must be handled with care. Compounds should not be heated when solid.) Anal. Calcd for C₁₀H₂₄N₆Cl₂NiO₈: C, 26.21; H, 5.25; N, 12.23. Found: C, 26.2; H, 5.3; N, 12.3.

[Ni(cyclen)](NO₃)₂. A solution of Ni(NO₃)₂·6H₂O (1 mmol) in 5 cm³ of methanol was added to a boiling solution of cyclen (1 mmol) in methanol (25 cm³). The blue solution was reduced by heating (ca. 10 cm³), and 50 cm³ of hot butanol was added. On cooling, the complex

Table I. Crystallographic Data for [Ni₂(Me₂cyclen)₂ox](ClO₄)₂·2H₂O and [Ni(cyclen)(H₂O)₂]₂(C₄O₄)(ClO₄)₂

	1	3
formula	C ₂₂ H ₅₂ N ₈ Cl ₂ Ni ₂ O ₁₄	C ₂₀ H ₄₈ N ₈ Cl ₂ Ni ₂ O ₁₆
mol wt	840.5	854.0
space group	P2 ₁ /n	P2 ₁ cn
a, Å	22.815 (15)	11.124 (3)
b, Å	10.713 (1)	11.461 (3)
c, Å	7.506 (3)	25.735 (6)
β, deg	97.85 (3)	
V, Å ³	1817 (2)	3281.0 (4)
Z	2	4
temp, °C	25	25
λ, Å	0.71073	0.71073
ρ _{obsd} , g cm ⁻³	1.54	1.73
ρ _{calcd} , g cm ⁻³	1.53	1.71
μ, cm ⁻¹	13	14
R = Σ ΔF /Σ F _o	4.15	3.45
R _w = [Σw ΔF ² /ΣwF _o ²]	4.65	3.88

separated as a blue-mauve microcrystalline powder. The product was filtered, washed with ethanol and then with diethyl ether, and dried in vacuo. Anal. Calcd for C₈H₂₀N₆NiO₆: C, 26.93; H, 5.65; N, 23.55. Found: C, 27.1; H, 5.7; N, 23.7.

[Ni₂(Me₂cyclen)₂ox](ClO₄)₂·2H₂O (1). A 0.5-mmol sample of lithium oxalate dissolved in a minimum amount of water was added to a previously neutralized aqueous solution (50 cm³) of 1 mmol of Me₂cyclen·4HBr and 1 mmol of nickel(II) perchlorate hexahydrate. Dark blue prismatic crystals of 1 were obtained by slow evaporation of the resulting blue-violet solution at room temperature. They were filtered, washed with cold water, and dried over calcium chloride. Anal. Calcd for C₂₂H₅₂N₈Cl₂Ni₂O₁₄: C, 31.44; H, 6.19; N, 13.33. Found: C, 31.5; H, 5.9; N, 13.3.

[Ni₂(cyclen)₂ox](NO₃)₂ (2). [Ni(cyclen)](NO₃)₂ (1 mmol) and Na₂C₂O₄ (0.5 mmol) were dissolved in 20 cm³ of water, and the resulting solution was brought to pH 6–7 by addition of few drops of sodium hydroxide solution. When the volume of this solution was reduced at room temperature, a blue-violet microcrystalline powder of 2 was formed. The compound was filtered, washed with methanol, and dried in vacuo. Anal. Calcd for C₁₈H₄₀N₁₀Ni₂O₁₀: C, 32.08; H, 5.98; N, 20.78. Found: C, 32.0; H, 6.0; N, 20.8.

[Ni(cyclen)(H₂O)₂]₂(C₄O₄)(ClO₄)₂ (3). A 0.5-mmol sample of lithium squarate dissolved in a minimum amount of water was added to a warm solution of 1 mmol of 1,4,7,10-tetraazacyclododecane and 1 mmol of nickel(II) perchlorate hexahydrate (40 cm³). A mauve solution is obtained after heating at 80 °C under stirring for half an hour. Blue-violet plate-shaped crystals of 3 were obtained by slow evaporation of the solvent at room temperature. Anal. Calcd for C₂₂H₅₂N₈Cl₂Ni₂O₁₄: C, 31.44; H, 6.19; N, 13.33. Found: C, 31.5; H, 5.9; N, 13.3.

X-ray Data Collection and Structure Refinement. Diffraction data were collected on Phillips PW 1000 and CAD4 Enraf-Nonius diffractometers for compounds 1 and 3, respectively, using in both cases graphite-monochromated Mo Kα (λ = 0.71073 Å) radiation. Accurate unit cell parameters were obtained from least-squares refinement of 25 reflections in the 14–16 θ range. They are listed in Table I along with other relevant crystallographic details. A full-length table of crystallographic data is given in the supplementary material (Table S1). Two standard reflections were measured every 2 h, but no systematic loss of intensity was observed during the data collection. Intensity data were collected by the θ–2θ scan technique in the 2θ range 3–75°. No absorption correction was applied in the case of complex 1 as suggested by a flat Ψ scan, whereas for compound 3 an empirical absorption correction using the Ψ scan of two reflections was applied. The 2558 independent reflections having I ≥ 3σ(I) from a total of 3019 reflections for complex 1 (2059 and 3039 respectively for complex 3) were considered as observed and used in the structural analysis. The nickel atom of 1 was located on a Patterson map, and all other atoms were found on subsequent Fourier maps. All atoms, except hydrogen, had anisotropic thermal parameters. Hydrogen atoms were found on a difference map and refined with an overall isotropic thermal parameter. The structure of 3 was solved by direct methods. Least-squares refinements were carried out in seven blocks (434 parameters). All atoms, except hydrogen, had anisotropic thermal parameters. Some hydrogens were found from a difference map; all others were introduced in calculated positions, and they were not refined. The function minimized in both structures was Σw(|F_o| – |F_c|)², the weighting scheme being w = 1/Σ_{j=1,3} A_jT_j(X) with three coefficients (2.706, 0.326, 2.022 for 1 and 8.690, 0.001 and 5.657 for 3) for a Chebyshev series in which X = (F_o/F_c)_{max}.¹⁵ The atomic scattering factors,

- (4) Bosnich, B.; Tobe, M. L.; Webb, G. A. *Inorg. Chem.* **1965**, *4*, 1109.
- (5) Barefield, E. K.; Wagner, F.; Hodges, K. D. *Inorg. Chem.* **1976**, *15*, 1370.
- (6) Martin, L. Y.; Sperati, C. R.; Busch, D. H. *J. Am. Chem. Soc.* **1977**, *99*, 2968.
- (7) Fabbrizzi, L. *Inorg. Chim. Acta* **1977**, *24*, L21.
- (8) Busch, D. H. *Acc. Chem. Res.* **1978**, *11*, 392.
- (9) Billo, E. J. *Inorg. Chem.* **1981**, *20*, 4019.
- (10) Billo, E. J. *Inorg. Chem.* **1984**, *23*, 236.
- (11) Barefield, E. K.; Bianchi, A.; Billo, E. J.; Connolly, P. G.; Paoletti, P.; Summers, J. S.; Van Derveer, D. G. *Inorg. Chem.* **1986**, *25*, 4197.
- (12) Thöm, V. J.; Hancock, R. D. *J. Chem. Soc., Dalton Trans.* **1985**, 1877 and references therein.
- (13) Fabbrizzi, L.; Micheloni, M.; Paoletti, P. *Inorg. Chem.* **1980**, *19*, 535.
- (14) Ciampolini, M.; Micheloni, M.; Nardi, N.; Paoletti, P.; Dapporto, P.; Zanobini, F. *J. Chem. Soc., Dalton Trans.* **1984**, 1357.

Table II. Atomic Coordinates and Thermal Parameters^{a,b} for Non-Hydrogen Atoms of [Ni₂(Me₂cyclen)₂ox](ClO₄)₂·2H₂O

atom	<i>x/a</i>	<i>y/b</i>	<i>z/c</i>	<i>U</i> _{eq} , Å ²
Ni(1)	0.08259 (1)	0.10628 (4)	0.25264 (4)	0.0340
O(1)	0.06473 (9)	0.0796 (2)	-0.0260 (3)	0.0406
O(2)	0.00290 (8)	0.0056 (2)	0.2337 (2)	0.0371
O(3)	0.2367 (1)	0.3180 (3)	0.5384 (5)	0.0826
N(1)	0.0841 (1)	0.1138 (3)	0.5261 (3)	0.0411
N(2)	0.0472 (1)	0.2926 (3)	0.2543 (4)	0.0507
N(3)	0.1592 (1)	0.2020 (4)	0.2270 (4)	0.0523
N(4)	0.1435 (1)	-0.0461 (3)	0.3096 (4)	0.0530
C(1)	0.0782 (2)	0.2449 (4)	0.5772 (4)	0.0531
C(2)	0.0327 (2)	0.3066 (4)	0.4401 (5)	0.0600
C(3)	0.0951 (2)	0.3791 (4)	0.2191 (6)	0.0683
C(4)	0.1408 (2)	0.3099 (5)	0.1236 (6)	0.0685
C(5)	0.1975 (2)	0.1075 (6)	0.1565 (6)	0.0690
C(6)	0.2030 (2)	0.0002 (5)	0.2778 (6)	0.0675
C(7)	0.1424 (2)	-0.0719 (4)	0.5058 (5)	0.0631
C(8)	0.1368 (2)	0.0467 (4)	0.6094 (4)	0.0503
C(9)	0.0179 (1)	0.0212 (3)	-0.0750 (3)	0.0341
C(10)	-0.0067 (2)	0.3152 (4)	0.1220 (6)	0.0694
C(11)	0.1280 (2)	-0.1605 (5)	0.2046 (6)	0.0722
Cl(2)	0.16131 (6)	0.5818 (1)	0.7289 (2)	0.0784
O(10)	0.1555 (3)	0.6988 (6)	0.8138 (8)	0.109 (1) ^c
O(11)	0.2116 (5)	0.627 (1)	0.647 (1)	0.109 (1) ^c
O(12)	0.1110 (5)	0.498 (1)	0.759 (2)	0.109 (1) ^c
O(13)	0.1217 (6)	0.599 (1)	0.567 (2)	0.109 (1) ^c
O(14)	0.1632 (6)	0.632 (1)	0.906 (2)	0.109 (1) ^c
O(15)	0.1570 (6)	0.600 (1)	0.538 (2)	0.109 (1) ^c
O(16)	0.2189 (6)	0.546 (2)	0.719 (2)	0.109 (1) ^c
O(17)	0.1902 (7)	0.461 (1)	0.795 (2)	0.109 (1) ^c
O(18)	0.1107 (8)	0.542 (2)	0.648 (3)	0.109 (1) ^c
O(19)	0.2117 (9)	0.506 (2)	0.807 (3)	0.109 (1) ^c
O(20)	0.145 (1)	0.485 (2)	0.820 (3)	0.109 (1) ^c

^aNumbers in parentheses are estimated standard deviations in the last significant figure. ^b $U_{eq} = 1/3 \sum_i \sum_j (U_{ij} a_i^* a_j^* a_i a_j)$. ^cThese values correspond to U_{iso} .

corrected for anomalous dispersion, were from ref 16. All the calculations were performed by using a VAX 725 computer with SHELX-76,¹⁷ CRYSTALS,¹⁵ and ORTEP¹⁸ programs. The final values of discrepancy indices, *R* and *R*_w, were 4.15 and 4.65 for **1** and 3.45 and 3.88 for **3**, respectively. The final difference-Fourier maps show residual maxima and minima in the vicinity of the disordered perchlorate of +1.23 and -0.92 e Å⁻³ for **1** and of +0.38 and -0.31 e Å⁻³ for **3**. Refined positional parameters for non-hydrogen atoms of complexes **1** and **3** are given in Tables II and III, respectively. Anisotropic thermal parameters, positional parameters for hydrogen atoms, bond distances and angles concerning Me₂cyclen and cyclen ligands, and observed and calculated structure factors for both complexes (Tables S2-S9) are available as supplementary material.

Spectroscopic and Magnetic Measurements. Infrared spectra were recorded on a Perkin-Elmer 1750 FTIR spectrophotometer as KBr pellets. The electronic spectra were performed on a Perkin-Elmer Lambda 9 spectrometer equipped with 1-cm cells thermostated at 25 °C. The diffuse reflectance spectra were also recorded with the same apparatus as Nujol mulls on filter paper. Magnetic susceptibility measurements were carried out on polycrystalline samples in the 300-4.2 K temperature range by means of a pendulum-type apparatus¹⁹ equipped with a helium cryostat. Mercury tetrakis(thiocyanato)cobaltate(II) was used as a susceptibility standard. Corrections for the diamagnetism of complexes **1** and **2** were estimated from Pascal's constants as -434 × 10⁻⁶ and -353 × 10⁻⁶ cm³ mol⁻¹ respectively. Magnetic susceptibility data were also corrected for TIP (-100 × 10⁻⁶ cm³ mol⁻¹ per nickel(II) ion).

Emf Measurements. The potentiometric titrations were carried out, in 0.1 mol dm⁻³ KNO₃ solution at 25 °C, by using equipment (potentiometer, cell, buret, stirrer, microcomputer, etc.) that has been fully

Table III. Atomic Coordinates and Thermal Parameters^{a,c} for Non-Hydrogen Atoms of [Ni(cyclen)(H₂O)₂]₂(C₄O₄)(ClO₄)₂

atom	<i>x/a</i>	<i>y/b</i>	<i>z/c</i>	<i>U</i> _{eq} , Å ²
Ni(1)	0.2752	0.85853 (4)	0.37268 (2)	0.0215
O(1)	0.3869 (7)	0.7754 (7)	0.3206 (3)	0.0279
O(2)	0.1320 (9)	0.7802 (7)	0.3217 (4)	0.335
N(1)	0.256 (1)	0.7315 (3)	0.4325 (1)	0.0277
N(2)	0.1177 (8)	0.9228 (8)	0.4133 (3)	0.0288
N(3)	0.265 (1)	1.0261 (3)	0.3391 (1)	0.0256
N(4)	0.4086 (8)	0.9228 (8)	0.4141 (4)	0.0188
C(1)	0.144 (1)	0.746 (1)	0.4626 (5)	0.0360
C(2)	0.105 (1)	0.869 (1)	0.4668 (5)	0.0334
C(3)	0.111 (1)	1.0542 (9)	0.4108 (5)	0.0275
C(4)	0.1457 (8)	1.0869 (9)	0.3586 (5)	0.0197
C(5)	0.371 (1)	1.083 (1)	0.3538 (6)	0.0398
C(6)	0.408 (1)	1.048 (1)	0.4109 (6)	0.0319
C(7)	0.404 (1)	0.878 (1)	0.4659 (5)	0.0281
C(8)	0.367 (1)	0.748 (1)	0.4644 (5)	0.0353
Ni'(1)	0.2571 (2)	0.00138 (4)	0.17788 (1)	0.0209
O'(1)	0.3789 (8)	0.0741 (8)	0.2326 (3)	0.0352
O'(2)	0.1355 (7)	0.0691 (7)	0.2316 (3)	0.0201
N'(1)	0.260 (1)	-0.1765 (3)	0.2023 (1)	0.0262
N'(2)	0.4027 (8)	-0.0544 (8)	0.1339 (4)	0.0290
N'(3)	0.266 (1)	0.1439 (3)	0.1264 (1)	0.0242
N'(4)	0.1084 (9)	-0.0511 (8)	0.1339 (4)	0.0242
C'(1)	0.368 (1)	-0.2285 (8)	0.1809 (4)	0.0223
C'(2)	0.407 (1)	-0.176 (1)	0.1306 (5)	0.0235
C'(3)	0.411 (1)	0.0104 (8)	0.0862 (5)	0.0339
C'(4)	0.362 (1)	0.135 (1)	0.0945 (5)	0.0257
C'(5)	0.137 (1)	0.141 (1)	0.0965 (6)	0.0345
C'(6)	0.111 (1)	0.014 (1)	0.0837 (5)	0.0302
C'(7)	0.108 (1)	-0.1841 (8)	0.1294 (5)	0.0260
C'(8)	0.142 (1)	-0.233 (1)	0.1837 (5)	0.0346
O(10)	0.1096 (7)	0.3070 (7)	0.2310 (3)	0.0208
O(11)	0.3999 (8)	0.3015 (7)	0.2331 (4)	0.0411
O(12)	0.4034 (7)	0.5573 (7)	0.2876 (4)	0.0295
O(13)	0.1147 (6)	0.5530 (7)	0.2904 (3)	0.0311
C(10)	0.191 (1)	0.3744 (9)	0.2469 (5)	0.0285
C(11)	0.3232 (9)	0.3725 (8)	0.2470 (4)	0.0153
C(12)	0.320 (1)	0.4876 (7)	0.2734 (4)	0.0178
C(13)	0.1898 (9)	0.485 (1)	0.2722 (5)	0.0235
Cl(1)	0.2595 (4)	1.03310 (9)	0.59709 (4)	0.0404
O(3)	0.268 (1)	0.9138 (3)	0.5844 (2)	0.0585
O(4)	0.277 (2)	1.0940 (4)	0.5504 (2)	0.0839
O(5)	0.3544 (9)	1.073 (1)	0.6248 (5)	0.0758
O(6)	0.1532 (9)	1.054 (2)	0.6299 (5)	0.0765
Cl'(1)	0.2579 (6)	0.3903 (1)	0.43750 (5)	0.0539
O'(3)	0.3095 (9)	0.437 (1)	0.3917 (3)	0.1329
O'(4)	0.344 (1)	0.319 (1)	0.436 (1)	0.1241
O'(5)	0.281 (2)	0.4794 (4)	0.4706 (2)	0.0828
O'(6)	0.1494 (8)	0.325 (1)	0.4571 (4)	0.0901

^aNumbers in parentheses are estimated standard deviations in the last significant figure. ^b $U_{eq} = 1/3 \sum_i \sum_j (U_{ij} a_i^* a_j^* a_i a_j)$. ^cPrimed atoms refer to the atoms of the other crystallographically independent mononuclear unit.

described.²⁰ The reference electrode was an Ag/AgCl electrode in saturated KCl solution. The glass electrode was calibrated as a hydrogen concentration probe by titrating well-known amounts of HCl with CO₂-free NaOH solutions and determining the equivalent point by the Gran method,²¹ which gives the standard potential of the cell, *E*⁰, and the ionic product of water. The computer program SUPERQUAD²² was used to calculate the stability constants. The equilibria involving [Ni(cyclen)]²⁺ or [Ni(Me₂cyclen)]²⁺ and ox²⁻ have been first investigated by titrating solutions containing the nickel(II) complexes with oxalic acid standard solutions. Furthermore, out-of-cell batchwise titrations were performed for both systems in order to check for the attainment of the equilibria. The measurements carried out by both methods were consistent, leading to the same values of stability constants for the mononuclear complexes [Ni(cyclen)ox] and [Ni(Me₂cyclen)ox]. As is known, tetrazamacrocyclic nickel(II) complexes are inert enough, with respect

- (15) Carruthers, J. R.; Watkin, D. W. J. CRYSTALS. An advanced crystallographic computer program. Chemical Crystallography Laboratory, University of Oxford, 1985.
- (16) *International Tables for X-ray Crystallography*; Kynoch Press: Birmingham, England, 1974; Vol. IV, Table 2.3.1.
- (17) Sheldrick, G. M. SHELX-76. Program for crystal structure determination. University Chemical Laboratory, Cambridge, England, 1986.
- (18) Johnson, C. K.; ORTEP. Report ORNL-3794; Oak Ridge National Laboratory: Oak Ridge, TN, 1965.
- (19) Bernier, J. C.; Poix, P. *Actual. Chim.* **1978**, 2, 7.

- (20) Bianchi, A.; Bologni, L.; Dapporto, P.; Micheloni, M.; Paoletti, P. *Inorg. Chem.* **1984**, 23, 1201.
- (21) Gran, G. *Analyst (London)* **1952**, 77, 661. Rossotti, F. J.; Rossotti, H. *J. Chem. Educ.* **1965**, 42, 375.
- (22) Gans, P.; Sabatini, A.; Vacca, A. *J. Chem. Soc., Dalton Trans.* **1985**, 1195.

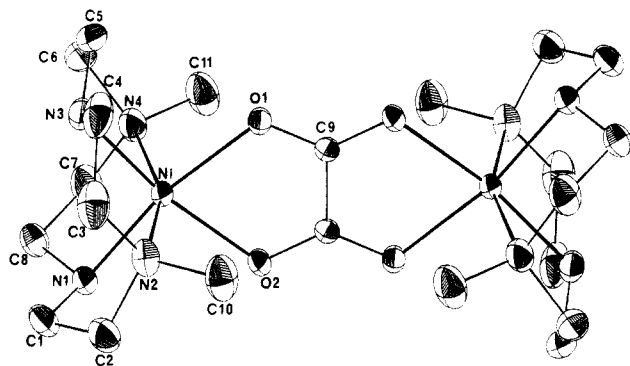


Figure 1. ORTEP drawing of the $[\text{Ni}_2(\text{Me}_2\text{cyclen})_2\text{ox}]^{2+}$ binuclear cation. Hydrogen atoms are not shown for the sake of clarity. Probability ellipsoids are 30%.

to acid dissociation, to allow the performance of these measurements. Nevertheless, aqueous solutions of these complexes buffered at acid pH (3–4) were spectrophotometrically tested for acid decomposition over the period of the potentiometric titrations. Although further measurements were carried out by titrating aqueous solutions of $[\text{Ni}_2(\text{cyclen})_2\text{ox}](\text{NO}_3)_2$ and $[\text{Ni}_2(\text{Me}_2\text{cyclen})_2\text{ox}](\text{ClO}_4)_2 \cdot 2\text{H}_2\text{O}$ with oxalic acid, only the stability constants of the mononuclear complexes could be determined.

The interaction of these nickel(II) macrocyclic complexes with squarate anion has been also studied by the methods indicated above, but no mixed-ligand complexes were detected.

Microcalorimetry. The enthalpies of reaction between oxalate anion and the nickel(II) complexes $[\text{Ni}(\text{L})]^{2+}$ (L = cyclam, cyclen, Me_2cyclen) to produce the mixed-ligand $[\text{Ni}(\text{L})\text{ox}]$ complexes have been determined in a 0.1 mol dm^{-3} KNO_3 , 0.05 mol dm^{-3} sodium tetraborate (pH = 9.6) water solution by means of a fully automatized piece of equipment having a Thermal Activity Monitor 2277 Model (Termometric AB) microcalorimeter as calorimetric unit. The system was programmed to follow calorimetric batchwise titrations. In a typical experiment, 2 cm^3 of oxalate solution buffered at pH = 9.6 by 0.05 mol dm^{-3} sodium tetraborate was placed into the calorimetric cell, and this solution was titrated with successive additions (addition volumes ranging from 40 to 100 μL) of $[\text{Ni}(\text{L})](\text{NO}_3)_2$ solution also buffered at pH = 9.6. All solutions were prepared in order to achieve a final 0.1 mol dm^{-3} KNO_3 concentration. The thermal effect produced by each addition was recorded and subsequently corrected, for the heats of dilution of the reacting solutions, by blank experiments. The heat evolution in the reactions of oxalate anion with the complexes $[\text{Ni}(\text{cyclen})]^{2+}$ and $[\text{Ni}(\text{Me}_2\text{cyclen})]^{2+}$ takes place within a few minutes. Twenty-four experimental points from four different experiments have been used to determine the enthalpies of these reactions. The heat evolution in the reaction of oxalate with $[\text{Ni}(\text{cyclam})]^{2+}$ takes place over a period of 8 h, as expected on the basis of previous kinetic studies.³ Ten different experiments consisting of a single addition were carried out to determine this enthalpy. On the basis of the equilibrium constants determined in this work for the formation of the mixed-ligand complexes $[\text{Ni}(\text{cyclen})\text{ox}]$ and $[\text{Ni}(\text{Me}_2\text{cyclen})\text{ox}]$ and those previously reported for $[\text{Ni}(\text{cyclam})]^{2+}$,² the composition of the reaction solution after each addition was calculated to verify the completion of the reactions.

Results and Discussion

Description of the Structures. $[\text{Ni}_2(\text{Me}_2\text{cyclen})_2\text{ox}](\text{ClO}_4)_2 \cdot 2\text{H}_2\text{O}$ (**1**). The crystal structure of **1** consists of $[\text{Ni}_2(\text{Me}_2\text{cyclen})_2\text{ox}]^{2+}$ binuclear cations, noncoordinated disordered perchlorate anions, and lattice water molecules. The tetradentate tetraazamacrocyclic ligand adopts a folded conformation to produce a cis-pseudooctahedral geometry at each nickel atom with the bis-bidentate oxalato bridge linking the two nickel atoms. A perspective view of the binuclear entity with the atom-labeling scheme and a stereoscopic view of the unit cell are shown in Figures 1 and 2, respectively. A symmetry center stands at the middle of the $\text{C}(9)\text{--}\text{C}(9)^i$ ($i = \bar{x}, \bar{y}, \bar{z}$) bond of the oxalato bridge. Main bond distances and angles of complex **1** are given in Table IV. The intramolecular $\text{Ni}\cdots\text{Ni}$ separation is 5.465 (1) Å, whereas the shortest intermolecular $\text{Ni}\cdots\text{Ni}$ distance is 6.083 (1) Å. The coordination around the metal ion is distorted octahedral. The significant difference between the $\text{Ni}\text{--}\text{N}(\text{secondary})$ and the $\text{Ni}\text{--}\text{N}(\text{tertiary})$ distances is noticeable (2.050 (2) and 2.059 (3) Å for $\text{Ni}(1)\text{--}\text{N}(1)$ and $\text{Ni}(1)\text{--}\text{N}(3)$ against 2.154 (3) and 2.148 (3) Å for $\text{Ni}(1)\text{--}\text{N}(2)$ and $\text{Ni}(1)\text{--}\text{N}(4)$, respectively). This structural feature had been

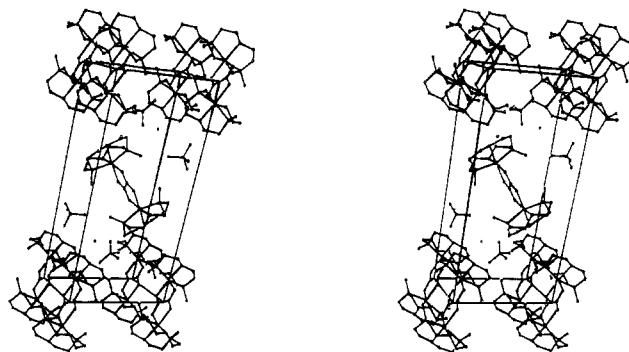


Figure 2. Stereoscopic view of the cell of $[\text{Ni}_2(\text{Me}_2\text{cyclen})_2\text{ox}](\text{ClO}_4)_2 \cdot 2\text{H}_2\text{O}$ down the c axis (the a axis is vertical).

Table IV. Selected Bond Distances (Å) and Angles (deg)^{a,b} for $[\text{Ni}_2(\text{Me}_2\text{cyclen})_2\text{ox}](\text{ClO}_4)_2 \cdot 2\text{H}_2\text{O}$

Distances			
Ni(1)–O(1)	2.095 (2)	Ni(1)–O(2)	2.102 (2)
Ni(1)–N(1)	2.050 (2)	Ni(1)–N(2)	2.154 (3)
Ni(1)–N(3)	2.059 (3)	Ni(1)–N(4)	2.148 (3)
O(1)–C(9)	1.249 (3)	O(2)–C(9 ⁱ)	1.254 (3)
C(9)–C(9 ⁱ)	1.547 (5)		
Angles			
O(2)–Ni(1)–O(1)	79.28 (7)	N(1)–Ni(1)–O(1)	168.35 (9)
N(1)–Ni(1)–O(2)	89.08 (8)	N(2)–Ni(1)–O(1)	96.3 (1)
N(2)–Ni(1)–O(2)	98.9 (1)	N(2)–Ni(1)–N(1)	85.0 (1)
N(3)–Ni(1)–O(1)	91.51 (9)	N(3)–Ni(1)–O(2)	170.79 (9)
N(3)–Ni(1)–N(1)	100.1 (1)	N(3)–Ni(1)–N(2)	82.1 (1)
N(4)–Ni(1)–O(1)	97.3 (1)	N(4)–Ni(1)–O(2)	98.8 (1)
N(4)–Ni(1)–N(1)	84.8 (1)	N(4)–Ni(1)–N(2)	159.4 (1)
N(4)–Ni(1)–N(3)	82.1 (1)	C(9)–O(1)–Ni(1)	113.8 (2)
C(9 ⁱ)–O(2)–Ni(1)	113.2 (2)	O(2 ⁱ)–C(9)–O(1)	126.3 (2)
C(9 ⁱ)–C(9)–O(1)	116.6 (3)	C(9 ⁱ)–C(9)–O(2 ⁱ)	117.1 (3)

^a Numbers in parentheses are estimated standard deviations in the last significant figure. ^b $i = \bar{x}, \bar{y}, \bar{z}$.

observed in the structure of the parent complex *cis*- $[\text{Ni}(\text{Me}_2\text{cyclen})(\text{H}_2\text{O})\text{Br}]\text{Br}$.¹⁴ The two Ni–O bond lengths (2.095 (2) and 2.102 (2) Å for Ni–O(1) and Ni–O(2), respectively) are slightly longer than the reported ones for the binuclear complex $[\text{Ni}_2(\text{cyclam})_2\text{ox}](\text{NO}_3)_2$.² The values of the N–Ni–N angles illustrate the distortion of the octahedron around nickel: they lie between 82.1 (1) and 85.0 (1)° for the five-membered rings, being 100.1 (1) and 159.4 (1)° for N(1)–Ni(1)–N(3) and N(2)–Ni(1)–N(4), respectively. These two last values reveal that the tetraaza ligand is unable to accommodate the present geometry entirely satisfactorily, leading to significant deviations from the ideal values of the angles, as has been observed in the bromide compound. The O(1)–Ni(1)–O(2) angle (79.28 (7)°) is very close to the reported ones for the other three μ -oxalato-bridged nickel(II) binuclear complexes.^{2,23} However, it is smaller than the Br(1)–Ni(1)–O(1) angle (82.5 (3)°) found in the above-mentioned bromide complex. The short bite distance of the oxalate ion (O(1)–O(2) 2.677 (3) Å) is at the origin of this difference. The N–C and C–C bond lengths agree well with the values reported for the same ligand in the bromide complex. However, an important difference is observed between both complexes when regarding the configuration of the four nitrogen atoms of the macrocycle: the four terminal groups of the nitrogen atoms, two hydrogens and two methyls, are on the same side with respect to the idealized macrocyclic plane in the bromide complex whereas only one hydrogen and the two methyls are on the same side in the structure of **1**. The chelate N–Ni–N rings are all in an asymmetric configuration and show the envelope conformation. Bond distances and angles in the oxalate ion are in the range expected and very close to those found in other compounds. The

(23) (a) Alcock, N. W.; Moore, P.; Omar, H. A. A. *Acta Crystallogr.* **1987**, *C43* (11), 2074. (b) Ribas, J.; Monfort, M.; Diaz, C.; Solans, X. *An. Quim.* **1988**, *B84*, 186.

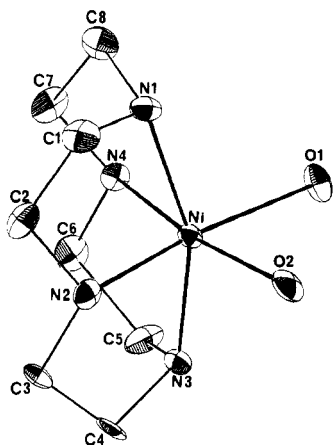


Figure 3. ORTEP drawing of the $[\text{Ni}(\text{cyclen})(\text{H}_2\text{O})_2]^{2+}$ cation. Hydrogen atoms are not shown for the sake of clarity. Probability ellipsoids are 30%.

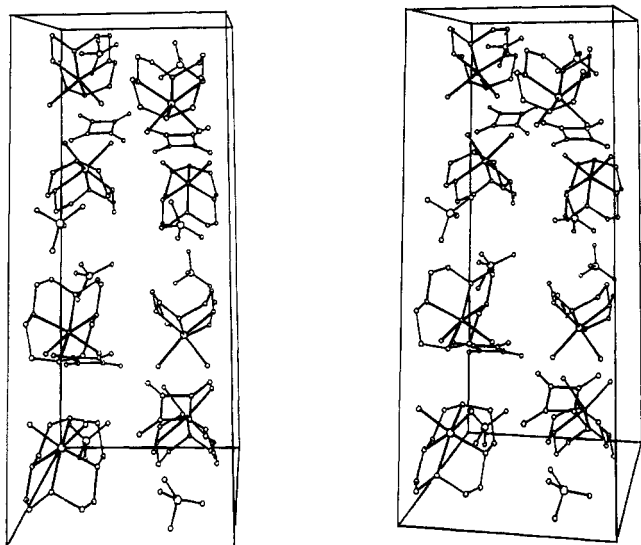


Figure 4. Stereoscopic view of the cell of $[\text{Ni}(\text{cyclen})(\text{H}_2\text{O})_2]^{2+}(\text{C}_4\text{O}_4)(\text{ClO}_4)_2$ down the b axis (the c axis is vertical).

oxalate group is planar^{2,23,24} and the nickel(II) ion lies only 0.02 Å out of this plane. Distances ranging from 2.78 to 2.95 Å are observed between the oxygen atoms of water molecules and disordered oxygen atoms of perchlorate groups. These hydrogen-bonding interactions have not been characterized because of the unsolved disorder of the perchlorate groups.

$[\text{Ni}(\text{cyclen})(\text{H}_2\text{O})_2]^{2+}(\text{C}_4\text{O}_4)(\text{ClO}_4)_2$ (3). The asymmetric unit is made up of two cationic groups of formula $[\text{Ni}(\text{cyclen})(\text{H}_2\text{O})_2]^{2+}$, one squarate anion, and two perchlorate anions. The two perchlorate groups are virtually identical although crystallographically independent. The tetradentate cyclen is folded so that the water molecules can be accommodated in cis positions. A perspective view of the cationic species along with the atom-labeling scheme and a stereoscopic view of the unit cell are depicted in Figures 3 and 4, respectively. The configuration of the four nitrogen atoms of the macrocycle is such that their hydrogen atoms are on the same side with respect to the idealized macrocyclic plane. The four five-membered chelate rings are in the asymmetric

Table V. Selected Bond Distances (Å) and Angles (deg)^{a,b} for $[\text{Ni}(\text{cyclen})(\text{H}_2\text{O})_2]^{2+}(\text{C}_4\text{O}_4)(\text{ClO}_4)_2$

Distances			
Ni(1)–N(1)	2.119 (4)	Ni'(1)–N'(1)	2.134 (3)
Ni(1)–N(2)	2.01 (1)	Ni'(1)–N'(2)	2.077 (9)
Ni(1)–N(3)	2.1069 (5)	Ni'(1)–N'(3)	2.105 (4)
Ni(1)–N(4)	2.124 (9)	Ni'(1)–N'(4)	2.09 (1)
Ni(1)–O(1)	2.187 (7)	Ni'(1)–O'(1)	2.124 (9)
Ni(1)–O(2)	2.113 (9)	Ni'(1)–O'(2)	2.083 (8)
C(10)–C(11)	1.467 (6)	C(10)–C(13)	1.42 (2)
C(10)–O(10)	1.26 (1)	C(11)–C(12)	1.49 (1)
C(11)–O(11)	1.23 (1)	C(12)–C(13)	1.452 (6)
C(12)–O(12)	1.28 (1)	C(13)–O(13)	1.24 (1)
Angles			
N(2)–Ni(1)–N(1)	82.4 (4)	N'(2)–Ni'(1)–N'(1)	81.7 (4)
N(3)–Ni(1)–N(1)	157.51 (9)	N'(3)–Ni'(1)–N'(1)	157.8 (2)
N(3)–Ni(1)–N(2)	84.8 (3)	N'(3)–Ni'(1)–N'(2)	81.9 (4)
N(4)–Ni(1)–N(1)	83.1 (4)	N'(4)–Ni'(1)–N'(1)	84.1 (4)
N(4)–Ni(1)–N(2)	102.9 (1)	N'(4)–Ni'(1)–N'(2)	103.5 (1)
N(4)–Ni(1)–N(3)	81.9 (3)	N'(4)–Ni'(1)–N'(3)	85.3 (4)
O(1)–Ni(1)–N(1)	98.7 (4)	O'(1)–Ni'(1)–N'(1)	99.8 (3)
O(1)–Ni(1)–N(2)	170.8 (3)	O'(1)–Ni'(1)–N'(2)	89.1 (4)
O(1)–Ni(1)–N(3)	96.9 (2)	O'(1)–Ni'(1)–N'(3)	94.8 (3)
O(1)–Ni(1)–N(4)	86.3 (4)	O'(1)–Ni'(1)–N'(4)	167.3 (4)
O(2)–Ni(1)–N(1)	98.9 (3)	O'(2)–Ni'(1)–N'(1)	99.8 (3)
O(2)–Ni(1)–N(2)	88.3 (4)	O'(1)–Ni'(1)–N'(2)	169.2 (3)
O(2)–Ni(1)–N(3)	99.1 (2)	O'(1)–Ni'(1)–N'(3)	99.1 (3)
O(2)–Ni(1)–N(4)	168.8 (4)	O'(1)–Ni'(1)–N'(4)	87.3 (4)
O(2)–Ni(1)–O(1)	82.5 (1)	O'(2)–Ni'(1)–O'(1)	80.1 (1)
C(13)–C(10)–C(11)	91.4 (10)	O(10)–C(10)–C(11)	135.4 (11)
O(10)–C(10)–C(13)	133.2 (11)	C(12)–C(11)–C(10)	88.0 (10)
O(11)–C(11)–C(10)	134.6 (12)	O(11)–C(11)–C(12)	137.3 (10)
C(13)–C(12)–C(11)	89.6 (10)	C(12)–C(12)–C(11)	132.2 (10)
C(12)–C(13)–C(10)	99.0 (10)	O(12)–C(12)–C(13)	138.2 (11)
O(13)–C(13)–C(12)	138.8 (12)	O(13)–C(13)–C(10)	138.0 (11)

^aNumbers in parentheses are estimated standard deviations in the last significant figure. ^bPrimed atoms refer to the atoms of the other crystallographically independent mononuclear unit.

configuration and have an envelope form. Two other structures in which this macrocycle is folded were reported some years ago.²⁵ Main bond distances and angles of the asymmetric unit are given in Table V. It should be noted that differences are observed in the Ni–N bond distances as well as in the Ni–O bond lengths. The angles around the nickel atoms show distortions with respect to those of a regular octahedron with N(2)–Ni(1)–N(4) expanded to 102.9 (1)° (N'(2)–Ni'(1)–N'(4) is 103.5 (1)°), and N(1)–Ni(1)–N(3) reduced to 81.9 (3)° (N'(1)–Ni'(1)–N'(3) is 85.3 (4)°). The O(1)–Ni(1)–O(2) angle is 82.5 (1)° (O'(1)–Ni'(1)–O'(2) is 80.1 (1)°). This value is smaller than the related O(1)–Ni(1)–O(2) angle observed in the previously described structure. In spite of these distortions, it could be considered that an approximate 2-fold axis bisects the O(1)–Ni(1)–O(2) and N(2)–Ni(1)–N(4) angles. The values of the N–Ni–N angles in the five-membered rings vary between 81.9 (3) and 84.8 (3)° (81.7 (4) and 85.3 (4)° for the other cationic species), and they are very close to the reported ones for the oxalato structure. The N–C and C–C bond lengths agree well with the values observed for the parent Me₂cyclen in the oxalato and bromide complexes.

The squarate anion is planar (the largest deviation is 0.051 Å for O(13)). The average C–C bond length (1.46 (1) Å) is very close to the mean values found in squaric acid (1.456 (12) Å)²⁶ and K₂C₄O₄·H₂O (1.457 (8) Å)²⁷ and slightly smaller than the values reported for Ni(C₄O₄)·2H₂O (1.487 (16) Å),²⁸ Ni(C₄O₄)(HIm)(H₂O)₂ (1.467 (2) Å),²⁹ and Ni(C₄O₄)(bpy)(H₂O)₂·2H₂O (1.460 (6) Å).³⁰ The O–C–C angles, varying

(24) (a) Hodgson, D. J.; Ibers, G. *Acta Crystallogr.* **1969**, *B25*, 469. (b) Curtis, N.; Ross, I.; McCormick, N.; Waters, N. *J. Chem. Soc., Dalton Trans.* **1973**, 1537. (c) Felthouse, T. R.; Laskowski, E. J.; Hendrickson, D. N. *Inorg. Chem.* **1977**, *16*, 1077. (d) Sletten, J. *Acta Chem. Scand.* **1983**, *A37*, 569. (e) Julve, M.; Verdager, M.; Gleizes, A.; Philoche-Levisalles, M.; Kahn, O. *Inorg. Chem.* **1984**, *23*, 3808. (f) Julve, M.; Faus, J.; Verdager, M.; Gleizes, A. *J. Am. Chem. Soc.* **1984**, *106*, 8306. (g) Bencini, A.; Fabretti, A. C.; Zanchini, C.; Zanini, P. *Inorg. Chem.* **1987**, *26*, 1445. (h) Castro, I.; Faus, J.; Julve, M.; Mollar, M.; Monge, A.; Gutiérrez-Puebla, E. *Inorg. Chim. Acta* **1989**, *161*, 97.

(25) (a) Iitaka, Y.; Shina, M.; Kimura, E. *Inorg. Chem.* **1974**, *13*, 2886. (b) Loehlin, J. H.; Fleisher, E. B. *Acta Crystallogr.* **1976**, *B32*, 3063. (26) Semmingsen, D. *Acta Chem. Scand.* **1973**, *27*, 3961. (27) MacIntyre, W. M.; Werkema, M. S. *J. Chem. Phys.* **1964**, *42*, 3563. (28) Habenschuss, M.; Gerstein, B. C. *J. Chem. Phys.* **1974**, *61*, 852. (29) Van Ooijen, J. A. C.; Reedijk, J.; Spek, A. L. *Inorg. Chem.* **1979**, *18*, 1184.

Table VI. Distances (Å) and Angles (deg) in the Interactions of the Type D-H...A (D = Donor; A = Acceptor) for $[\text{Ni}(\text{cyclen})(\text{H}_2\text{O})_2]_2(\text{C}_4\text{O}_4)(\text{ClO}_4)_2$

D	H	A	receptor atom position ^a	H...A ^b	D...A	D-H...A ^b
O(1)	H(5)	O(12)	x, y, z	1.57	2.646 (1)	169.3
O(1)	H(6) ^c	O(10)	$1/2 + x, 1/2 + y, 1/2 - z$	2.12	2.83 (1)	
O(2)	H(8)	O(13)	x, y, z	1.73	2.73 (1)	168.2
O(2)	H(7)	O(11)	$x - 1/2, 1/2 + y, 1/2 - z$	2.12	2.95 (1)	161.3
O'(1)	H'(6)	O(13)	$1/2 + x, y - 1/2, 1/2 - z$	1.80	2.70 (1)	171.8
O'(1)	H'(5)	O(11)	x, y, z	1.54	2.62 (1)	164.3
O'(2)	H'(7)	O(12)	$x - 1/2, y - 1/2, 1/2 - z$	1.79	2.63 (1)	170.5
O'(2)	H'(8)	O(10)	x, y, z	1.72	2.74 (1)	149.8

^aSymmetry operations applied to coordinates of Table III. ^bStandard deviations are not given because hydrogen atoms were not refined. ^cThis hydrogen atom has not been located.

between 130.8 (12) and 138.0 (11)°, exhibit a somewhat wider range than the reported ones for the mentioned squarate compounds. The C-C-C angles are very close to 90° and they range from 88.0 (10) to 91.4 (10)° (88.2 and 91.8° in squaric acid). Of particular interest in this structure is the presence of an extended network of strong hydrogen bonds between oxygen atoms of the squarate anion and coordinated water molecules. The relevant data are listed in Table VI. As a result of hydrogen bonding, squarate links cationic species forming sheets parallel to the *ab* plane as shown in Figure 4. The Ni-Ni' separation is 5.274 (1) Å.

Electronic and IR Spectra. The reflectance spectra of 1-3 are typical of those for d^8 configurations in near-octahedral ligand fields, exhibiting the three spin-allowed transitions from $^3A_{2g}$ to $^3T_{2g}$, $^3T_{1g}$, and $^3T_{1g}(P)$ as maxima at the frequencies given in Table VII. The first transition yields the octahedral splitting parameter, Δ_o , which in all these cases is smaller than the observed one for the complex $[\text{Ni}_2(\text{cyclam})_2\text{ox}](\text{NO}_3)_2$. The values of the nephelauxetic ratio, β , which are shown in Table VII, have been obtained for the octahedral case by calculation in the strong field coupling scheme with a d^8 configuration (considering $15B = 15840 \text{ cm}^{-1}$ for the gaseous ion (3P) for Ni^{2+}). A shoulder is also clearly detectable in the reflectance spectra at ca. 12350, 12650, and 12500 cm^{-1} for 1, 2, and 3, respectively. This feature could be attributed to the spin-forbidden $A_{2g}-E_g$ transition in O_h symmetry.

The infrared spectra of 1 and 2 exhibit the bands characteristic of the bridging oxalate ligand ($\nu_{\text{as}}(\text{CO})$ at 1650-1640 cm^{-1} , $\nu_{\text{s}}(\text{CO})$ at 1360 and 1312-1315 cm^{-1} and $\nu(\text{OCO})$ at 795 cm^{-1}).² As far as the IR spectrum of 3 is concerned, the most relevant features associated to the squarate ligand are a strong and broad absorption band centered at 1470 cm^{-1} ($\nu(\text{CO}) + \nu(\text{CC})$)³¹ and two weak peaks at 1600 cm^{-1} ($\nu(\text{CC})$) and 1750 cm^{-1} ($\nu(\text{CO})$).³² The IR spectra in the N-H stretching region for these three complexes consist of three peaks of medium-weak intensity (see Table VII). Three peaks (3160, 3220, and 3240 cm^{-1}) are also observed in this region for the complex $[\text{Ni}(\text{Me}_2\text{cyclen})(\text{H}_2\text{O})\text{Br}]\text{Br}\cdot\text{H}_2\text{O}$, in which the tetraazamacrocycle is folded. However, only a single $\nu(\text{NH})$ peak, which is centered at 3230 cm^{-1} , is present in the IR spectra of the yellow complex $[\text{Ni}(\text{Me}_2\text{cyclen})](\text{ClO}_4)_2$. Taking into account that a planar arrangement of the macrocycle occurs in this latter complex, it can be inferred that N-H stretching peaks could be used as diagnostic of cis or trans coordination. On the other hand, the similarity of IR spectra of complexes 2 and 3 regarding the N-H stretching region together with the presence of an oxalato bridge in complex 2 enables us to conclude that the cyclen ligand in such a complex is in a folded conformation. Its magnetic behavior supports this conclusion. The spectra of

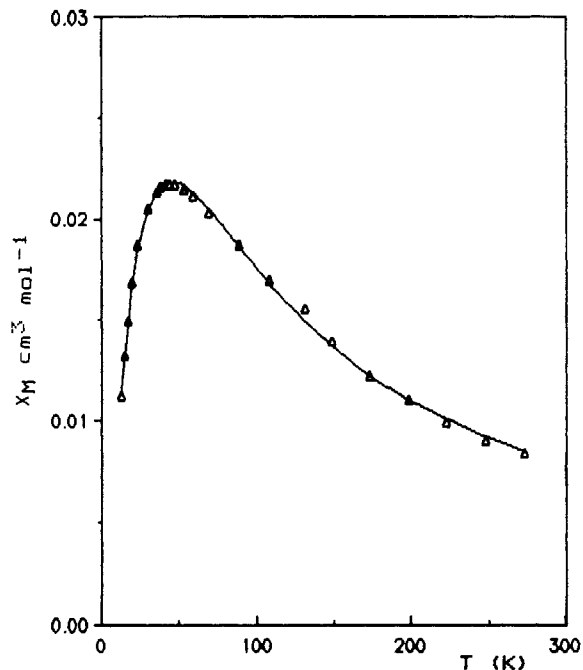


Figure 5. Plot of χ_M vs T for the complex $[\text{Ni}_2(\text{Me}_2\text{cyclen})_2\text{ox}](\text{ClO}_4)_2\cdot 2\text{H}_2\text{O}$. The solid line represents the theoretical values whereas triangles correspond to the experimental points.

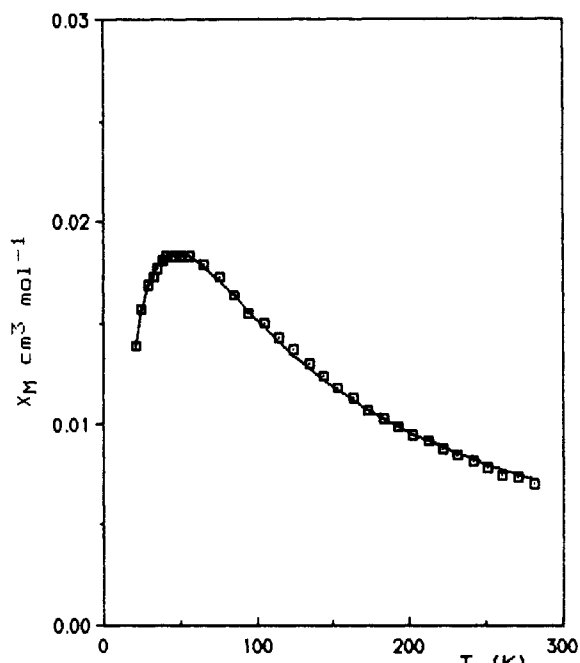


Figure 6. Plot of χ_M vs T for the complex $[\text{Ni}_2(\text{cyclen})_2\text{ox}](\text{NO}_3)_2$. The solid line represents the theoretical values whereas squares correspond to the experimental points.

complex 1 and 3 exhibit intense broad O-H stretching vibrations at 3420 and 3500 cm^{-1} for 1 and at 3600 and 3400 cm^{-1} for 3 that are indicative of hydrogen bonding.

Magnetic Properties. The molar magnetic susceptibility χ_M vs temperature curves for 1 and 2 are depicted in Figures 5 and 6. It can be seen that, at room temperature, χ_M has the value expected for two $S = 1$ states. The susceptibility curve for these compounds increases when the compound is cooled down until a maximum is reached at 47.4 and 53 K for 1 and 2, respectively, and then decreases markedly. This behavior is characteristic of an intramolecular antiferromagnetic interaction between two single-ion triplet states. As the ground state of nickel(II) in an octahedral environment is orbitally nondegenerate, the intramolecular exchange interaction can be represented by the isotropic

(30) Soules, R.; Dahan, F.; Laurent, J. P.; Castan, P. *J. Chem. Soc., Dalton Trans.* **1988**, 587.

(31) West, R.; Niu, H. Y. *J. Am. Chem. Soc.* **1963**, *85*, 2589.

(32) Wroblewski, J. T.; Brown, D. *Inorg. Chem.* **1978**, *17*, 2959.

Table VII. Infrared and Electronic Spectral Data for Complexes 1-3^{a,b}

compd	infrared peaks			reflectance spectral data				ref
	$\nu(\text{NH})^c$	$\nu(\text{CO})$		${}^3A_{2g} \rightarrow {}^3T_{2g}$	${}^3A_{2g} \rightarrow {}^3T_{1g}(\text{F})$	${}^3A_{2g} \rightarrow {}^3T_{1g}(\text{P})$	β	
$[\text{Ni}_2(\text{Me}_2\text{cyclen})_2\text{ox}](\text{ClO}_4)_2 \cdot 2\text{H}_2\text{O}$	3160 m, 3220 m, 3240 m	1640 s, 1360 m, 1315 m		10 500 br	17 500	28 570	0.893	this work
$[\text{Ni}_2(\text{cyclen})_2\text{ox}](\text{NO}_3)_2$	3250 m, 3270 m, 3290 m	1650 s, 1360 m, 1320 w		10 750 br	18 000	28 170	0.832	this work
$[\text{Ni}(\text{cyclen})(\text{H}_2\text{O})_2]_2(\text{C}_4\text{O}_4)(\text{ClO}_4)_2$	3260 m, 3290 m, 3310 m	1750 w, 1480 s, br		10 650 br	17 500	27 780	0.814	this work
$[\text{Ni}_2(\text{cyclam})_2\text{ox}](\text{NO}_3)_2$	3180 m, 3200 m, 3225 m	1650 s, 1360 m, 1315 w		11 500 br	18 500	29 400	0.831	2

^a Values for spectral data are given in cm^{-1} . The nephelauxetic ratio, β , is unitless. ^b s, m, w, and br stand for strong, medium, weak, and broad, respectively. ^c $\nu(\text{NH})$ for secondary amino group.

spin Hamiltonian $\hat{H} = -J\hat{S}_A \cdot \hat{S}_B$ where J is the exchange integral and $S_A = S_B = 1$ (local spins). χ_M may be expressed as

$$\chi_M = \frac{2N\beta^2 g^2}{kT} \left(\frac{\exp(J/kT) + 5 \exp(3J/kT)}{1 + \exp(J/kT) + 5 \exp(3J/kT)} \right) (1 - \rho) + \frac{2N\beta^2 g^2}{3kT} \rho$$

In this expression N , β , k , and T have their usual meanings. The last term accounts for the uncoupled nickel(II) impurity. We have not considered the effects of single-ion zero-field interactions on the magnetic susceptibility of these binuclear nickel(II) complexes because it has been shown that the zero-field splitting, D , does not change the position of the maximum.³³ It is well-known that this position determines the value of J ; therefore, D has little effect on the evaluation of J . The effect of D on the magnetic behavior can be neglected due to the large stabilization of the singlet ground state.

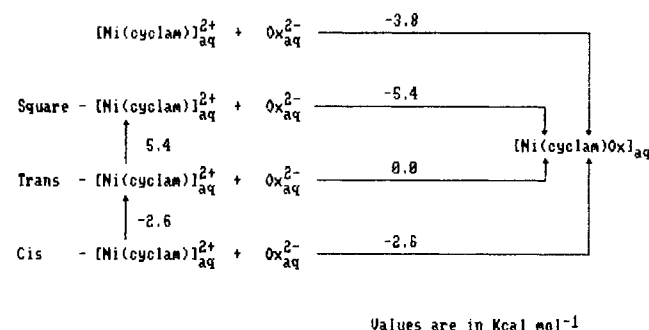
Least-squares fitting of all experimental points leads to J , g , and ρ values of -34 cm^{-1} , 2.30, and 0.048 for **1** and -35 cm^{-1} , 2.15, and 0.039 for **2**. The agreement factor $R = \sum (\chi_{\text{exptl}}(i) - \chi_{\text{calcd}}(i))^2 / \sum (\chi_{\text{exptl}}(i))^2$ is 1.45×10^{-4} for **1** and 7.59×10^{-5} for **2**. Previously reported J values for μ -oxalato-bridged nickel(II) binuclear complexes^{2,23b,33,34} are close to those of **1** and **2**. The large antiferromagnetic coupling observed is due to the strong overlap between the xy -type magnetic orbitals centered on the metal ions (x and y axis are defined by the M-O (oxalate) bonds), which are delocalized toward the oxygen atom of the oxalate bridge.³⁵ Such a situation has been found in linear chains^{35a,36} as well as in binuclear complexes involving first-row transition-metal ions.^{2,23b,24c,e-h,37}

One of the aims of the present work was to compare the ability of planar oxalate and squarate bridging ligands to transmit exchange interactions between two nickel(II) ions. It was found³³ that the interaction through the squarate was much smaller than the one through the oxalate for such a system. Two main reasons were given to explain this result: (i) squarate is larger than oxalate, and (ii) on the basis of a bis-bidentate coordination of both ligands toward metal ions, calculation on them showed that in the case of squarate the appropriate symmetry bridge orbitals lie at lower energy than those in oxalate. Nevertheless, the lack of crystal structure determinations for these complexes does not allow one to check the outlined symmetry considerations. In our case, efforts to grow single crystals of an oxalate and a related squarate complex have been successful and their structures have been determined. The oxalate acts in a bis-bidentate fashion, but unfortunately the squarate complex in the parent complex acts only as a counterion and consequently such a comparison remains an open question.

Table VIII. Thermodynamic Parameters for the Reaction of Oxalate Anion with $[\text{Ni}(\text{cyclen})]^{2+}$, $[\text{Ni}(\text{Me}_2\text{cyclen})]^{2+}$, and $[\text{Ni}(\text{cyclam})]^{2+}$ in a 0.1 mol dm^{-3} KNO_3 Aqueous Solution at 25 °C

reaction	ΔG° , kcal/mol	ΔH° , kcal/mol	$T\Delta S^\circ$, kcal/mol
$[\text{Ni}(\text{cyclen})]^{2+}(\text{aq}) + \text{ox}^{2-}(\text{aq})$	-5.6 (1) ^a	-2.4 (1)	3.2
$[\text{Ni}(\text{Me}_2\text{cyclen})]^{2+}(\text{aq}) + \text{ox}^{2-}(\text{aq})$	-5.7 (1)	-2.9 (1)	2.8
$[\text{Ni}(\text{cyclam})]^{2+}(\text{aq}) + \text{ox}^{2-}(\text{aq})$	-3.8 (1) ^b	-3.8 (1)	0.0
<i>cis</i> - $[\text{Ni}(\text{cyclam})]^{2+}(\text{aq}) + \text{ox}^{2-}(\text{aq})$	-6.1	-2.6	3.5
<i>trans</i> - $[\text{Ni}(\text{cyclam})]^{2+}(\text{aq}) + \text{ox}^{2-}(\text{aq})$	-4.5	0.0	4.5
<i>square</i> - $[\text{Ni}(\text{cyclam})]^{2+}(\text{aq}) + \text{ox}^{2-}(\text{aq})$	-4.0	-5.4	-1.4

^a Values in parentheses are standard deviations in the last significant figure. ^b Taken from ref 2. $[\text{Ni}(\text{cyclam})]^{2+}(\text{aq})$ is a mixture of planar (69%), *trans*-diaquo octahedral (29%) and *cis*-diaquo octahedral (2%) forms.

Scheme I

Thermodynamic Study. The thermodynamic parameters related to the equilibria between the oxalate anion and the nickel(II) complexes of cyclam, cyclen and Me_2cyclen in aqueous solution are reported in Table VIII.

The equilibrium constants for the reaction of formation of the complexes $[\text{Ni}(\text{cyclam})\text{ox}]$ and $[\text{Ni}_2(\text{cyclam})_2\text{ox}]^{2+}$ from $[\text{Ni}(\text{cyclam})]^{2+}$ and oxalate anion were determined by spectrophotometry.² The equilibrium $[\text{Ni}(\text{cyclam})]^{2+} + \text{ox}^{2-} = [\text{Ni}(\text{cyclam})\text{ox}]$ is slowly reached, being the rate law for the forward reaction $k_f = 13[\text{OH}^-] \text{ s}^{-1}$.³ For this reason, in the present work, the enthalpy change for the reaction of addition of the oxalate anion to the $[\text{Ni}(\text{cyclam})]^{2+}$ complex has been determined by a batch microcalorimetric technique in aqueous solutions buffered at pH = 9.6 (see Experimental Section). Under the experimental conditions employed, the heats of reaction have been detected within 8 h, which corresponds to the time required for the almost complete formation ($\approx 98\%$) of the $[\text{Ni}(\text{cyclam})\text{ox}]$ present at equilibrium. The enthalpy change obtained ($-3.8 (1) \text{ kcal mol}^{-1}$) is referred to the $[\text{Ni}(\text{cyclam})]^{2+}$ reacting solutions composed of square (69%), *trans*-diaquo (29%), and *cis*-diaquo (2%) forms.¹¹ From the enthalpies of interconversion between the three forms,¹¹ the enthalpic contribution to the addition of ox^{2-} to each one of these can be readily calculated (Scheme I). In the case of $[\text{Ni}(\text{cyclen})]^{2+}$ and $[\text{Ni}(\text{Me}_2\text{cyclen})]^{2+}$, the reactions with the oxalate anion are fast being the equilibrium reached on the time scale of a common potentiometric titration (see Experimental Section). This result agrees with the calorimetric measurements since only a few minutes were required for the calorimeter

- (33) Duggan, M. D.; Barefield, E. K.; Hendrickson, D. N. *Inorg. Chem.* **1973**, *12*, 985.
 (34) Ball, P. W.; Blake, A. B. *J. Chem. Soc. A* **1969**, 1415.
 (35) (a) Michalowicz, A.; Girerd, J. J.; Goulon, J. *Inorg. Chem.* **1979**, *18*, 3004. (b) Girerd, J. J.; Kahn, O.; Verdaguer, M. *Inorg. Chem.* **1980**, *19*, 274.
 (36) Verdaguer, M.; Julve, M.; Michalowicz, A.; Kahn, O. *Inorg. Chem.* **1983**, *22*, 2624.
 (37) (a) Bencini, A.; Benelli, C.; Gatteschi, D.; Zanchini, C. *Inorg. Chim. Acta* **1984**, *86*, 169. (b) Julve, M.; Kahn, O. *Inorg. Chim. Acta* **1983**, *76*, L39.

equilibration after the beginning of the reaction.

In contrast with the results obtained for $[\text{Ni}(\text{cyclam})]^{2+}$,² the formation of binuclear $[\text{Ni}_2(\text{L})_2\text{ox}]^{2+}$ (L = cyclen and Me_2cyclen) complexes in water solution has not been detected, under the experimental conditions employed, although these complexes have been isolated as crystalline compounds from aqueous solutions. The free energy changes for the reaction of $[\text{Ni}(\text{cyclen})]^{2+}$ and $[\text{Ni}(\text{Me}_2\text{cyclen})]^{2+}$ with the oxalate anion are equal, within experimental error, and are somewhat smaller than that observed for the analogous *cis*-diaquonickel(II) complex of cyclam (Table VIII). The equilibrium constant for the reaction $[\text{Ni}(\text{cyclam})\text{ox}] + [\text{Ni}(\text{cyclam})]^{2+} = [\text{Ni}_2(\text{cyclam})_2\text{ox}]^{2+}$ is very small ($\log K = 1.6$),² and even lower values could be expected for the analogous reactions involving the two 12-membered tetraazamacrocycles. So, $[\text{Ni}_2(\text{cyclen})_2\text{ox}]^{2+}$ and $[\text{Ni}_2(\text{Me}_2\text{cyclen})_2\text{ox}]^{2+}$ could be formed in solution, though in undetectable concentrations.

As shown in Table VIII, the reactions of oxalate ion with the *cis*-diaquo complexes are exothermic. Both enthalpy and entropy changes contribute similarly to the formation of $[\text{Ni}(\text{Me}_2\text{cyclen})\text{ox}]$, while the formation of $[\text{Ni}(\text{cyclen})\text{ox}]$ and $[\text{Ni}(\text{cyclam})\text{ox}]$ present mainly an entropic nature. In the case of $[\text{Ni}(\text{Me}_2\text{cyclen})\text{ox}]$ the greatest enthalpy and lowest entropy changes are observed. This can be explained by means of solvation effects. As shown by the molecular structures of both 12-membered macrocyclic complexes herein reported, the substituents (hydrogens or methyl groups) on the nitrogen atoms point toward the same side of the macrocyclic ring. Therefore, a different solvation in $[\text{Ni}(\text{cyclen})]^{2+}$ and $[\text{Ni}(\text{Me}_2\text{cyclen})]^{2+}$ in solution is to be expected. The presence of the methyl substituents will reduce the formation of hydrogen bonds between the nitrogen atoms of the ligand, the coordinated water molecules, and the solvent, yielding then a smaller desolvation on coordination of the oxalate ion.

Different thermodynamic behaviors can be observed for the addition of ox^{2-} to the three $[\text{Ni}(\text{cyclam})]^{2+}$ complexes in solution. The right disposition of the *cis* complex for the coordination of ox^{2-} (Chart I) is revealed by the greater free energy change, which is due to both favorable enthalpic and entropic contributions. In contrast, the spontaneity of the addition of the bidentate oxalato ligand to the *trans*-diaquo isomer is only due to the entropy change, as this reaction is almost athermic. The heat evolved in the substitution of the two water molecules by the oxalate ion is counterbalanced by that required for the complex to reach the folded conformation. The highest enthalpy term is observed for the coordination of ox^{2-} to the square $[\text{Ni}(\text{cyclam})]^{2+}$ complex, which does not require heat absorption for the detachment of coordinated water molecules. On the other hand, the reduction in the number of molecules occurring in this reaction gives rise to an unfavorable entropic contribution.

All the entropic contributions derived from the different forms compensate between them in such a way that the resulting entropic term for the addition of oxalate to the mixture of $[\text{Ni}(\text{cyclam})]^{2+}$ in solution is negligible.

Acknowledgment. This work was partially supported by the Spanish Comisión Interministerial de Ciencia y Tecnología (Proyecto PB85-0190) and the Italian Ministero della Pubblica Istruzione. We are indebted to Dr. Andrea Caneschi for magnetic data collection.

Supplementary Material Available: Listings of crystallographic parameters (Table S1), anisotropic thermal parameters (Tables S2 and S3), hydrogen coordinates (Tables S4 and S5), and nonessential bond angles and distances (Tables S6 and S7) (9 pages); listings of calculated and observed structure factors (Tables S8 and S9) (34 pages). Magnetic data are available on request from the authors. Ordering information is given on any current masthead page.

Contribution No. 5012 from E. I. du Pont de Nemours & Company, Central Research & Development Department, Experimental Station, P.O. Box 80328, Wilmington, Delaware 19880-0328

Electronic and Molecular Structure of $[\text{FKrNCH}]^+$. The Question of Hypervalent Bonding

David A. Dixon* and Anthony J. Arduengo, III

Received February 22, 1989

The molecular structure of $[\text{KrFNCH}]^+$ has been calculated by using ab initio molecular orbital theory. The force field was calculated, and the molecule is predicted to be linear. Reasonable agreement with the two observed vibrational Raman bands in the solid is found. The stretching mode leading to dissociation into $[\text{KrF}]^+$ and NCH is calculated to be near 200 cm^{-1} . The $[\text{KrF}]^+$ and NCH fragments in the complex have geometries similar to those for the isolated molecules. The Kr—N bond distance is predicted to be quite short, 2.32 \AA . The complex $[\text{FKrNCH}]^+$ is predicted to be bound by 38.6 kcal/mol with respect to $[\text{KrF}]^+$ and NCH at the MP-2 level (30.2 kcal/mol , SCF level) with zero-point energy corrections. This is much higher than the 16.6 kcal/mol found at the SCF level for the Rb^+ complex with NCH, which corresponds to a purely ionic complex. All of the calculated results are consistent with an ionic and a covalent component in the bonding of $[\text{FKr}]^+$ with NCH. The molecular orbitals and bonding are analyzed in terms of three-center and four-center hypervalent bonds. Both types of hypervalent bonds are expected to play a role in the description of the covalent σ -bonding in $[\text{FKrNCH}]^+$. The charge distribution for $[\text{FKrNCH}]^+$ shows some transfer of electronic charge from the carbon to the $[\text{KrF}]^+$ region, consistent with some contribution from the resonance structure $\text{F}^--\text{Kr}^+=\text{N}=\text{C}^+-\text{H}$.

Introduction

The electronic and molecular structures of "hypervalent" molecules are of continual fascination to chemists. Molecules that in a formal sense appear to violate the Lewis octet rule are intriguing and help to provide us with new insights into molecular structure and behavior. This is especially true when the atom involved as the hypervalent center is an atom from the first row of the periodic table ($n = 2$).¹ The presence of the hypervalent

bond, the three-center, four-electron (3c,4e) bond, has been used to explain the chemistry and bonding in a wide range of molecules.^{2,5} We have recently shown the presence of a 5c,6e hypervalent bond in $[\text{F}_2\text{I}-\text{F}-\text{I}-\text{R}_f]^{-1}$ complexes using a combination of experimental and theoretical techniques.⁶ We have extended

(1) (a) Ault, B. S.; Andrews, L. *J. Am. Chem. Soc.* **1976**, *98*, 1591; *Inorg. Chem.* **1977**, *16*, 2024. (b) Lee, D. Y.; Martin, J. C. *J. Am. Chem. Soc.* **1984**, *106*, 5745. (c) Forbus, T. R., Jr.; Martin, J. C. *J. Am. Chem. Soc.* **1979**, *101*, 5057.

(2) Musher, J. I. *Angew. Chem., Int. Ed. Engl.* **1969**, *8*, 54. Musher describes the hypervalent bond, the 3c,4e bond, in a valence-bond description based on the models of Pimentel³ and Rundle.⁴
 (3) Pimentel, G. C. *J. Chem. Phys.* **1951**, *19*, 446.
 (4) Rundle, R. E. *Surv. Prog. Chem.* **1963**, *1*, 81.
 (5) Cahill, P. A.; Dykstra, C. E.; Martin, J. C. *J. Am. Chem. Soc.* **1985**, *107*, 6359. These authors describe the hypervalent bond in simple molecular orbital terms following Musher's² valence-bond description.